THE JOURNAL OF COMPARATIVE NEUROLOGY 506:224–239 (2008)

Embryonic and Postnatal Development of Microglial Cells in the Mouse Retina

ANA M. SANTOS, RUTH CALVENTE, MOHAMED TASSI, MARIA-CARMEN CARRASCO, DAVID MARTÍN-OLIVA, JOSÉ L. MARÍN-TEVA, JULIO NAVASCUÉS, AND MIGUEL A. CUADROS*

Departamento de Biología Celular, Facultad de Ciencias, Universidad de Granada, E-18071 Granada, Spain

ABSTRACT

Macrophage/microglial cells in the mouse retina during embryonic and postnatal development were studied by immunocytochemistry with Iba1, F4/80, anti-CD45, and anti-CD68 antibodies and by tomato lectin histochemistry. These cells were already present in the retina of embryos aged 11.5 days (E11.5) in association with cell death. At E12.5 some macrophage/microglial cells also appeared in peripheral regions of the retina with no apparent relationship with cell death. Immediately before birth microglial cells were present in the neuroblastic, inner plexiform (IPL), and ganglion cell (GCL) layers, and their distribution suggested that they entered the retina from the ciliary margin and the vitreous. The density of retinal microglial cells strongly decreased at birth, increased during the first postnatal week as a consequence of the entry of microglial precursors into the retina from the vitreous, and subsequently decreased owing to the cessation of microglial entry and the increase in retina size. The mature topographical distribution pattern of microglia emerged during postnatal development of the retina, apparently by radial migration of microglial cells from the vitreal surface in a vitreal-to-scleral direction. Whereas microglial cells were only seen in the GCL and IPL at birth, they progressively appeared in more scleral layers at increasing postnatal ages. Thus, microglial cells were present within all layers of the retina except the outer nuclear layer at the beginning of the second postnatal week. Once microglial cells reached their definitive location, they progressively ramified. J. Comp. Neurol. 506:224–239, 2008.

Indexing terms: development; ameboid microglia; macrophage; cell death; vascularization

Microglial cells are involved in surveillance and cleaning of the central nervous system (CNS), in immune reactions in the nervous parenchyma, and probably also in the emergence of the mature organization of the CNS (Kreutzberg, 1996; Aloisi, 2001; Mallat et al., 2005). These cells adopt different morphological and immunophenotypical features in different situations. Immature microglial cells are frequent during embryonic and postnatal development. Most of them are ameboid cells (so-called ameboid microglia) and others show a primitive ramification. Mature microglial cells are fully ramified and were previously thought to be quiescent cells but recent studies have revealed them to be highly motile cells that continually survey their microenvironment by extension and retraction of processes (Nimmerjahn et al., 2005). Injury of CNS regions gives rise to the activation of ramified microglial cells, which acquire morphological and immunophenotypical features similar to macrophages (Streit et al., 1999). In addition, macrophages arising from monocytes of the blood circulation also invade the nervous parenchyma in many CNS injuries. Hence, it is frequently difficult to distinguish between activated microglial cells and peripheral macrophages (Stoll and Jander, 1999; Cuadros et al., 2000) and they are often designated as macrophage/microglial cells. The same term is also used to refer to cells of macrophage lineage that appear during early CNS development (Cuadros et al., 1993; Herbomel et

Grant sponsor: Spanish Ministry of Education and Science; Grant number: BFU2004-01209.

*Correspondence to: Miguel A. Cuadros, Departamento de Biología Celular, Facultad de Ciencias, Universidad de Granada, E-18071 Granada, Spain. E-mail: macuadro@ugr.es

Received 13 February 2007; Revised 21 June 2007; Accepted 11 September 2007

DOI 10.1002/cne.21538

Published online in Wiley InterScience (www.interscience.wiley.com).

TABLE 1. Antibodies Used

Antibody	Source	Type, Host	Dilution
Iba1	Wako Pure Chemicals, Osaka, Japan #019-19741	Polyclonal, rabbit	1:100-1:200
F4/80	Serotec, Oxford, UK, #MCA 497	Monoclonal, rat	1:30
CD45	Serotec #MCA 1388	Monoclonal, rat	1:40
CD68	Serotec #MCA 1957	Monoclonal, rat	1:40
Ki 67	Abcam, Cambridge, UK, #ab15580	Polyclonal, rabbit	1:100

al., 2001) and whose final fate is not evident: they might become microglia as development advances or might disappear and be substituted by true microglial precursors. In this study the term macrophage/microglial cells is used to refer to macrophage-lineage cells whose final fate is not clearly established, while the term microglial cells is reserved for cells whose fate can be unequivocally traced during development until they become microglial cells.

Microglia originate from cells of mesodermal lineage that colonize the CNS (Cuadros and Navascués, 1998), including the retina, to achieve a mature distribution pattern that is specific to each CNS region (Lawson et al., 1990; Mittelbronn et al., 2001). The distribution of microglial cells in the adult retina has been described in fish (Dowding et al., 1991; Salvador-Silva et al., 2000), amphibians (Goodbrand and Gaze, 1991), birds (Navascués et al., 1994; Won et al., 2000; Cuadros et al., 2006), and mammals, including rabbits (Ashwell, 1989; Schnitzer, 1989; Humphrey and Moore, 1996), mice (Zhang et al., 2005b), rats (Ashwell et al., 1989; Harada et al., 2002; Zhang et al., 2005a), monkeys (Vrabec, 1970; Boycott and Hopkins, 1981), and humans (Penfold et al., 1991, 2001; Provis et al., 1995; Yang et al., 2000; Gupta et al., 2003). It has been observed in these species that microglial cells in the adult normal retina appear in the ganglion cell layer (GCL) and all fibrous layers, whereas they are scarce in the inner nuclear layer (INL) and absent in the outer nuclear layer (ONL). Many studies have demonstrated that these cells respond to different injuries in the retina (Humphrey and Moore, 1996; Roque et al., 1996; Chen et al., 2002; Harada et al., 2002; Zhang et al., 2005a,b), modifying this normal distribution pattern.

Emergence of the microglial distribution pattern during development has been far less investigated than its final outcome in the adult retina and has been extensively studied at our laboratory in the quail (Navascués et al., 1994, 1995; Marín-Teva et al., 1998, 1999a,c; Sánchez-López et al., 2004). These studies revealed that microglial cells colonize the quail retina by two different forms of migration, tangential and radial. Microglial cells spread on the vitreal surface of the retina by tangential migration along the developing nerve fiber layer (NFL). Subsequently, microglial cells reach other retinal layers by radial migration. There are few data on microglial development in the retina of other species. Detailed reports have been published on the presence and distribution of microglia in the developing retina of rats (Ashwell et al., 1989) and rabbits (Ashwell, 1989; Schnitzer, 1989), while only some development stages have been studied in mice (Hume et al., 1983; Hughes et al., 2003) and humans (Diaz-Araya et al., 1995a,b). It has also been reported that the distribution of microglial cells differs between pigmented and albino mouse retinas (Ng and Streilein, 2001).

In the present study different microglial markers were used to characterize the sequence of changes in the distribution of microglial cells at each embryonic and postnatal developmental stage, comparing these changes between two different strains of mice (C57BL/6, pigmented, and BALB/c, albino).

MATERIALS AND METHODS

Animals and histology

One hundred fifty embryos and postnatal mice of different ages were used in this study. Two different strains of mice were provided by the Animal Experimentation Service of the University of Granada: C57BL/6 pigmented and BALB/c albino mice. The age of embryos was determined by checking the presence of a vaginal plug in pregnant females; the morning of the day of plug detection was considered day 0.5 of gestation on the assumption that gestation had commenced the previous night. Embryos aged from 11.5 days of gestation (E11.5) to E18.5 were obtained from pregnant females subjected to deep halothane anesthesia (Fluothane, AstraZeneca Farmaceútica, Pontevedra, Spain). Ages of postnatal animals studied ranged from day of birth (P0) to adulthood (P45–60). Embryos and early postnatal animals were killed by decapitation. Older animals were killed by cervical dislocation or anesthetic overdose. In all cases experimental procedures followed guidelines issued by the Research Ethics Committee of our university.

The fixatives used in this study were 4% paraformaldehyde in phosphate-buffered saline (PBS, pH 7.4), periodate-lysine-paraformaldehyde (PLP, Yamato et al., 1984), and Bouin's fluid. The entire head of embryos or enucleated eyes from postnatal animals were fixed in paraformaldehyde or PLP for 1–6 hours. Fixed material was cryoprotected in PBS (pH 7.4) containing 30% sucrose, soaked in OCT compound (Sakura Finitek Europe, Zoeterwoude, The Netherlands), and frozen in liquid nitrogen. Blocks were stored at −40°C until use. Twenty-μm-thick transverse sections of retinas were obtained in a cryostat (Leica, Wetzlar, Germany) and collected on Superfrost slides (Menzel-Glasser, Braunschweig, Germany). Additional embryo heads and postnatal eyes were fixed in Bouin's fluid for 15–24 hours and embedded in paraffin wax. Paraffin blocks were cut in a rotatory microtome (Leica) at 10-μm thickness.

Immunocytochemistry

The antibodies used in this study and their sources and dilutions are summarized in Table 1. The Iba1 antibody was raised against the C-terminal end (sequence PTGPPAKKAISELP) of the iba1 protein, a calcium-binding protein of macrophages and microglial cells present in rodents (Ito et al., 1998); this antibody recognizes a band of about 17 kDa on Western blot. F4/80 antibody binds to a surface glycoprotein of mouse macrophages and microglia

that have a mass of around 160 kDa in immunoprecipitation and Western blot experiments (Hume and Gordon, 1983; our unpubl. results); the immunogen was peritoneal activated macrophages from C57/BL mice. Anti-CD45 and anti-CD68 antibodies recognize mouse homologs of CD45 and CD68 molecules, respectively. CD45 is a tyrosine phosphatase protein present in the membrane of cells of monocyte/macrophage lineage (Penninger et al., 2001) and the antibody used, whose immunogen was purified B cells from mouse lymph nodes, recognizes a single band of >170 kDa in Western blot of mouse brain extracts (Cuadros et al., 2006). CD68 (macrosialin) is a membrane glycoprotein present in lysosomes of macrophage-lineage cells (Da Silva and Gordon, 1999); the antibody used in this study, raised against concavalin A acceptor protein from P815 cell line (manufacturer's technical information), recognizes bands of 87–115 kDa corresponding to different degrees of protein glycosylation related to cell activation and phagocytosis (Da Silva and Gordon, 1999). Finally, the immunogen for the Ki67 antibody was a peptide within residues 1200–1300 (sequence EDLAGFKELFQTP) of human Ki67 protein (manufacturer's technical information); it recognizes on Western blot a protein of 345–395 kDa present in the nucleus of proliferating cells (Schlüter et al., 1993; manufacturer's technical information) and is therefore used as a marker of cell proliferation. As negative control, primary antibodies were omitted in some sections, resulting in the abolition of immunostaining. In addition, immunolabeled cells showed the expected distribution and shape in immunostained sections. Thus, cells strongly labeled with Iba1, F4/80, anti-CD45, and anti-CD68 were observed within blood vessels, vitreous, and periocular tissues, showing the morphological features of monocytes/macrophages. Ki67 immunopositive cells appeared in proliferative regions of the retina and periocular tissues.

After permeabilization in 0.1% Triton X-100 (Sigma, St. Louis, MO) in PBS (pH 7.4), sections were incubated with normal goat serum (Sigma) diluted 1:30 in PBS–1% bovine serum albumin (PBS-BSA) for 45–60 minutes. Then they were incubated with the primary antibody for 30–48 hours at 4°C, washed in PBS, and incubated with the corresponding secondary antibody diluted 1:1,000 in PBS-BSA for 2–3 hours at room temperature. The secondary antibodies used were Cy3-conjugated goat antirabbit IgG (Amersham Biosciences, UK) for Iba1 and Ki67, and Alexa Fluor 488-conjugated goat antirat IgG (Molecular Probes, Eugene, OR) for the other primary antibodies. Sections were stained with Hoechst 33342 (Sigma) to label cell nuclei, washed, and mounted with Fluoromount G (Southern Biotech, Birmingham, AL).

Some sections were double-labeled with Iba1 and another antibody (F4/80, anti-CD45, or anti-CD68), by incubating with mixtures of the two primary and two secondary antibodies at the same concentrations and similar times as for single immunolabelings.

The extravidin-biotin peroxidase technique was used in some sections for visualizing the label. Endogen peroxidase activity was eliminated from these sections by incubating them with 0.3% hydrogen peroxide before their incubation with the primary antibody. After treatment with the corresponding biotinylated secondary antibody (either biotin-conjugated antirabbit IgG or biotin-conjugated antirat IgG, both from Sigma), sections were incubated with extravidin-peroxidase complex (Sigma) for 1 hour at room temperature. The presence of peroxidase was revealed by incubation with a diaminobenzidine solution, either with or without nickel enhancement. Finally, sections were counterstained with either hematoxylin or methyl green and coverslipped with DePeX (DHB, Poole, UK).

Lectin histochemistry and TUNEL staining

Some cryostat and paraffin sections were treated with tomato lectin (TL) histochemistry, which labels microglial cells within the CNS of rodents (Acarin et al., 1994). Cryostat sections were permeabilized with 0.2% Triton X-100 in 0.05 M Tris-buffered saline (TBS, pH 7.2) for 10 minutes, while paraffin sections were dewaxed in xylol. They were then incubated with biotin-conjugated TL (Sigma) diluted 1:10 in TBS with 0.1% Triton X-100 for 2 hours at 37°C. Sections were then washed in TBS without Triton and incubated in avidin complex conjugated with peroxidase, fluorescein isothiocyanate, or tetramethylrhodamine isothiocyanate (all three from Sigma) for 1 hour at room temperature. Peroxidase-labeled sections were developed with diaminobenzidine, counterstained with hematoxylin, dehydrated, and mounted in DePeX. Fluorescence-labeled sections were mounted with Fluoromount G (Southern Biotech) after nuclear staining with Hoechst 33342 (Sigma).

Some sections were double-labeled with TL and either Iba1 or Ki67 antibodies. In these preparations, Iba1 or Ki67 immunolabeling was performed first followed by TL histochemistry as described above.

To investigate the possible incidence of cell death in microglial cells, some sections were double-labeled using TL and the terminal deoxynucleotidyl transferase (TDT) dUTP nick-end labeling (TUNEL) technique. In these cases the TL histochemistry (see above) was performed before extensive washing in PBS and sections were subsequently incubated in a solution containing 2% of TDT (Promega, Madison, WI) in TDT buffer (Promega, pH 6.8) and 0.03% of tetramethylrhodamine-dUTP (Roche Diagnostics, Mannheim, Germany) for 1 hour at 37°C. After incubation, sections were washed with PBS, stained with nuclear dye Hoechst 33342 (Sigma), and mounted using Fluoromount G (Southern Biotech).

Microscopy and cell counting

Fluorescence- and peroxidase-labeled sections were observed under an AxioPhot microscope (Zeiss, Oberkochen, Germany), and micrographs were obtained with an AxioCam digital camera (Zeiss). Confocal microscope pictures were obtained using a Leitz DMRB microscope equipped with a Leica TCS-SP5 scanning laser confocal imaging system (Leica). In confocal microscopy studies stacks of horizontal (xy) optical sections of selected fields in retinal sections were collected at 0.5–1-μm intervals through the z-dimension. Leica confocal software was used to superimpose optical sections from each microscopic field onto projection images of microglial cells contained in the field. The images obtained using normal or confocal microscopy were stored in TIFF format and prepared digitally in Adobe Photoshop (Adobe Systems, San Jose, CA) by adjusting contrast and brightness.

Drawings of some retinas from peroxidase-labeled sections were made using a camera lucida attachment. Location of microglial cells within the retina were marked on these drawings. In order to obtain complete images of

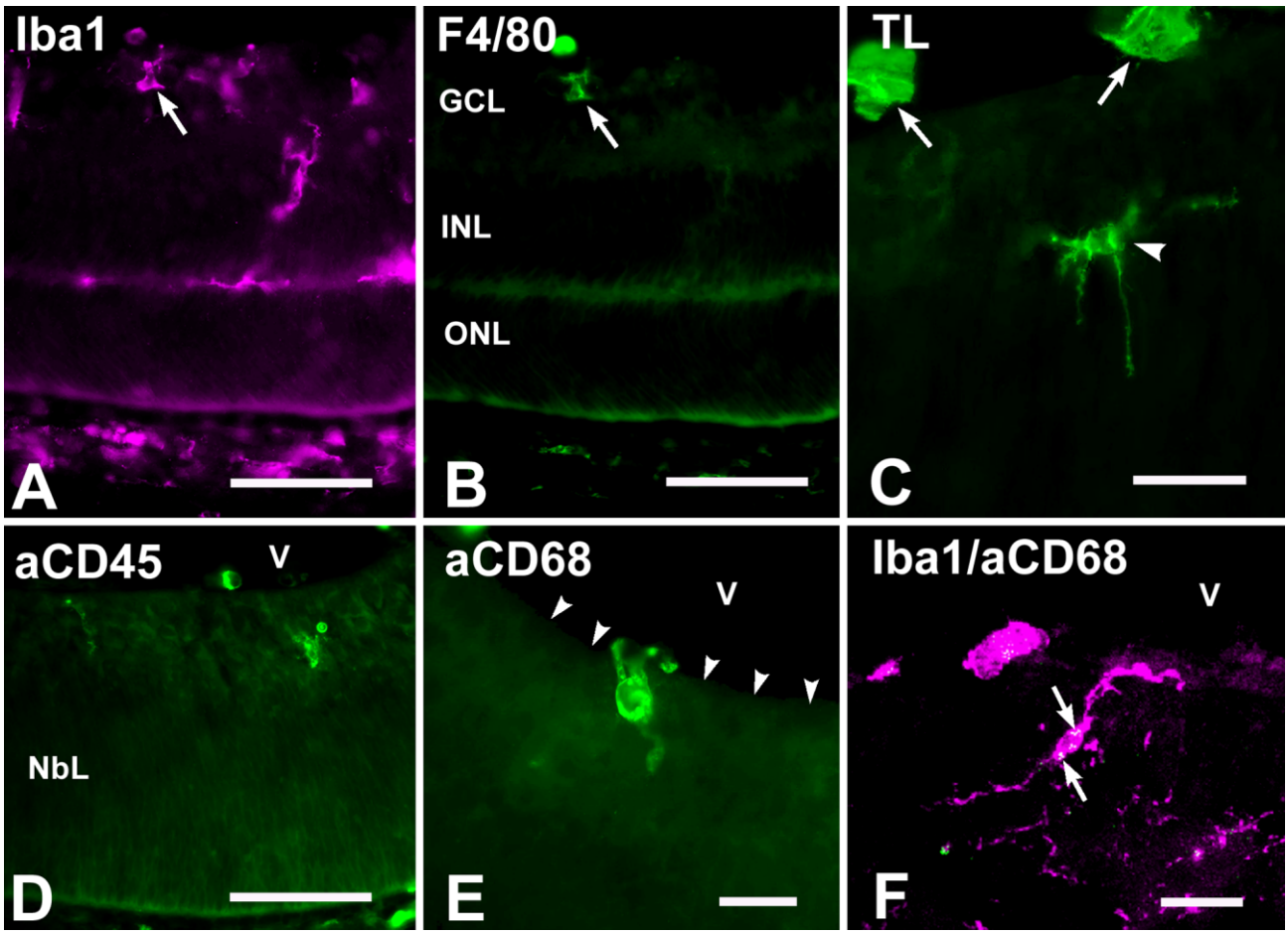

Fig. 1. Labeling of macrophage/microglial cells in developing mouse retinas by immunocytochemistry with different antibodies (A,B, D–F) and tomato lectin (TL) histochemistry (C). **A,B:** Double immunocytochemical labeling of a P7 retina section with antibodies Iba1 (magenta) and F4/80 (green). Numerous microglial cells are immunolabeled with Iba1 antibody, whereas only some of them (arrow) show F4/80 labeling. **C:** Histochemical labeling with TL of a microglia cell (arrowhead) in an E17.5 retina; arrows indicate labeled blood vessels in the vitreous. **D:** Very few microglial cells are labeled with antiCD45 antibody in an E18.5 retina, although Iba1 antibody revealed the presence of more microglial cells (not shown, but see Fig. 4A for Iba1 immunostaining of a retina of similar age). **E:** A microglial cell is strongly labeled with antiCD68 antibody and appears to be in the act of traversing the inner limiting membrane (arrowheads) in a P0 retina. **F:** Confocal microscope image of a microglial cell double-immunolabeled with Iba1 (magenta) and antiCD68 (green) antibodies in a P21 retina. AntiCD68 labeling is reduced to a few spots (arrows) reminiscent of lysosomes within the cell body. GCL, ganglion cell layer; INL, inner nuclear layer; ONL, outer nuclear layer; V, vitreous; NbL, neuroblastic layer. Scale bars = 20 μm in A–E; 35 μm in F.

some peroxidase-labeled cells, pictures taken at different levels of focus were combined by using ImageJ software (NIH, Bethesda, MD) supplied with the "Extended depth of field" plug-in created at the Swiss Federal Institute de Technology Lausanne (EPFL, Lausanne, Switzerland).

Microglial cells were counted in retinas from embryonic (E17.5 and E18.5) and postnatal (P0–P28) mice. Cell bodies displaying Iba1 immunoreactivity were counted in 20-μm-thick cryostat transverse retinal sections comprising both central and peripheral areas of the retina. Cells were only counted in every second section to avoid any double counting. At least four retinas from at least three animals were counted at each stage, and six different sections were counted in each retina. ImageJ (NIH) was used to measure the retinal surface in sections in order to estimate the density of Iba1-positive cells (number of labeled cells per μm^2) at each developmental age.

RESULTS

Differences in microglial labeling among the markers

We used different microglial markers in an attempt to label all microglial cells in our preparations. The Iba1 antibody appeared to be the most reliable marker of microglia during development and adulthood (Fig. 1A). Therefore, our study mainly relied on observations made from material immunostained with this antibody. No apparent differences in Iba1 labeling were observed between paraformaldehyde- and PLP-fixed retinas, whereas no labeling was detected after Bouin fixation.

The present findings for F4/80 antibody did not reproduce previously published studies, in which all microglial cells were apparently marked by this antibody throughout the brain and retina (Hume et al., 1983; Lawson et al., 1990) In our study, F4/80 labeling was similar to Iba1

labeling during the initial embryonic stages considered here (see Fig. 2) but then decreased. The decrease in F4/80 immunolabeling was seen in retinas fixed with any of the fixatives (Bouin's fluid, paraformaldehyde, or PLP). In late embryonic and postnatal retinas, F4/80 antibody recognized ameboid microglia but did not mark ramified cells, which were strongly labeled with Iba1 (compare Fig. 1A,B). A recent report (Hughes et al., 2003) described extensive labeling of retinal microglia with this antibody after fixation by perfusion. Although we have no definitive explanation for this discrepancy, it may be attributable to our use of fixation by immersion.

TL staining (Fig. 1C) gave comparable results to those obtained with Iba1 in embryonic and P0–10 retinas. The TL labeling of microglial cells decreased after P10, when blood vessels, also labeled by TL, invaded the retina. This made it difficult to determine whether specific labeling profiles corresponded to microglial cells. Therefore, TL proved to be a useful marker of microglial cells until P10 but gave inconclusive results at later ages.

Anti-CD45 antibody strongly labeled the macrophage/microglial cells present in the retina of E11.5–12.5 embryos but gave a weak labeling thereafter (Fig. 1D), despite the fact that strongly labeled cells continued to be seen in mesenchymal tissues surrounding the eye. PLP fixation improved the intensity of CD45 immunostaining.

Microglial labeling with anti-CD68 antibody frequently showed a dotted staining, as expected for a marker that recognizes a lysosomal component. This antibody strongly marked cells within the retina of E11.5–12.5 embryos and cells close to the vitreal border until the end of the first postnatal week (Fig. 1E). As development advanced, expression of the antigen recognized by this antibody appeared to be downregulated in cells localized at some distance from the vitreal border, and CD68 labeling was usually reduced to a few spots within the body of retinal microglial cells (Fig. 1F). This finding contrasted with the presence of strong immunolabeled cells outside the retina. PLP fixation improved the intensity of anti-CD68 immunostaining, as also found with anti-CD45.

Distribution of macrophage/microglial cells during embryonic development

Cells labeled with macrophage/microglial markers were already present in E11.5 retinas, mainly in their central regions (Fig. 2A), and they increased in number at E12.5 (Fig. 2B,C). Labeled cells were also present within the vitreous, both outside and inside blood vessels. Many labeled cells within the retina were macrophage-like cells, showing a rounded shape and frequently apoptotic bodies in their cytoplasm (Fig. 2D). At E12.5, macrophage-like cells were also seen at the peripheral retina (Fig. 2E). Rounded labeled cells containing cell debris were no longer present in the retina from E13.5 on, although labeled cells with ameboid profile or incipient ramification increased in number and became distributed throughout the retina between E13.5 and E15.5 (Figs. 2F–H, 3A).

From E16.5 on the GCL became segregated from the neuroblastic layer (NbL), and the IPL anlage appeared. Iba1-labeled cells were present in the IPL shortly after its emergence (Fig. 3B). Labeled cells were also present in the GCL and NbL (Figs. 3B, 4A). Iba1-labeled cells in the IPL and NbL of retinas at late embryonic development were poorly ramified cells, with a cell body and some broad processes emerging in different directions. Hence, their morphological features were very different from those of labeled cells in E11.5–12.5 retinas. In late embryonic retinas some Iba1-labeled cells were localized near or across the vitreal border of the retina (Fig. 3C), suggesting that they passed from the vitreous, where numerous labeled cells were seen, to the retinal parenchyma.

At the end of embryonic development, therefore, microglial cells were located in the NFL, GCL, IPL, and NbL (Fig. 4A).

Distribution of microglial cells during postnatal development

Many fewer microglial cells were present in P0 retinas than in retinas at the end of embryonic development (compare Fig. 4B with 4A). This was confirmed by determining the density of microglial (Iba1-positive) cells in the retina at different developmental stages. Microglial cell density in the mouse retina was reduced by around half between E18.5 and P0, although it increased again during the first postnatal week (Fig. 5A).

In order to determine whether the decrease in microglial cell density observed at birth was due to the death of microglial cells, we double-stained some sections from E18.5 embryos and P0 animals with TL, a microglial marker, and TUNEL, which labels degenerating cells. Although some TL-positive processes were apparently directed toward TUNEL-positive cell fragments, no microglial cell with TUNEL-positive nucleus was detected (Fig. 5B,C), suggesting that cell death does not decisively contribute to the perinatal decrease in the density of retinal microglia.

Numerous labeled cells were present at P0 in the NFL, GCL, and IPL, whereas very few labeled cells were observed in the NbL (Figs. 4B, 6A,B). This made it easier to monitor the migration of microglia from vitreal to scleral layers during subsequent development of the retina. Some microglial cells were located close to the vitreal border and others were seen across this border (Fig. 6C), suggesting that they were entering the retina from the vitreous. Many microglial cells at P0 were poorly ramified, with thick processes emerging from the cell body (Fig. 6A,B).

A clear change in the distribution of microglial cells was observed at P3 (Fig. 7A), with many Iba1-positive cells in the vitreal half of the NbL where almost none had been observed at P0. Labeled cells continued to be seen close to the vitreal border, as described at P0. Because microglial cell density increased during the first postnatal week, some sections of P0–7 retinas were double-labeled with TL and Ki67 (cell proliferation marker) to determine whether extensive proliferation of microglial cells occurs at this developmental time. In addition to labeling proliferating cells in the NbL of the retina, Ki67 also labeled endothelial cells and cells located outside the retina; however, no Ki67 labeling of microglial cell nuclei was found, indicating that retinal microglial cells were not proliferating (Fig. 5D,E).

At P7 the OPL became detectable within the NbL in central regions of the retina, allowing us to distinguish outer and inner nuclear layers. In regions with a well-defined ONL, microglial cells did not enter this layer but were localized throughout the other retinal layers (Fig. 7B). In contrast, microglial cells were observed in areas corresponding to the future ONL in retinal regions where the OPL had not differentiated (Fig. 7C). Far fewer labeled cells apparently penetrating the retina from the vitreous were observed at P7

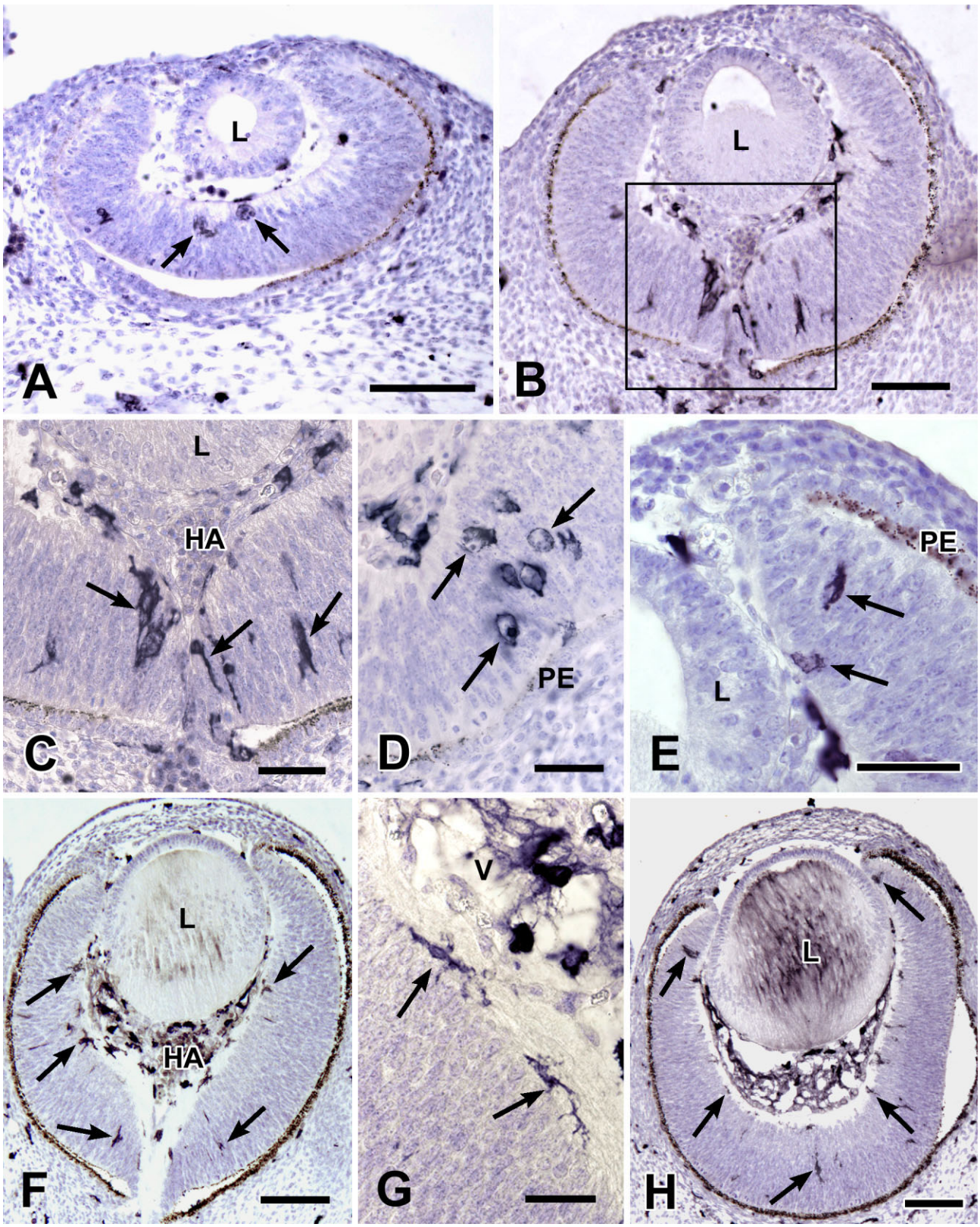

Fig. 2. F4/80 immunolabeling visualized with peroxidase in sections of E11.5–14.5 mouse retinas. **A:** Macrophage-like cells (arrows) in the central region of an E11.5 retina. **B:** F4/80 immunopositive cells in an E12.5 retina; the boxed area is shown at higher magnification in C. **C:** Region of the optic disk (boxed area in B) of an E12.5 retina, showing numerous F4/80-immunopositive macrophage/microglial cells (arrows). **D:** Rounded F4/80-immunopositive cells containing pyknotic bodies (some marked by arrows) in an E12.5 retina. **E:** F4/80-immunopositive cells (arrows) in the peripheral area of an E12.5 retina. **F:** F4/80-immunopositive cells (arrows) in central and peripheral areas of an E13.5 retina. **G:** Two immunolabeled cells (arrows) with ramified morphology located near the optic disk of an E13.5 retina. **H:** General view of an E14.5 eye showing F4/80-immunolabeled cells (some marked by arrows) throughout the retina. HA, hyaloid artery; L, lens primordium; PE, pigment epithelium; V, vitreous. Scale bars = 100 μm in A,B,F,H; 30 μm in C,D,G; 20 μm in E.

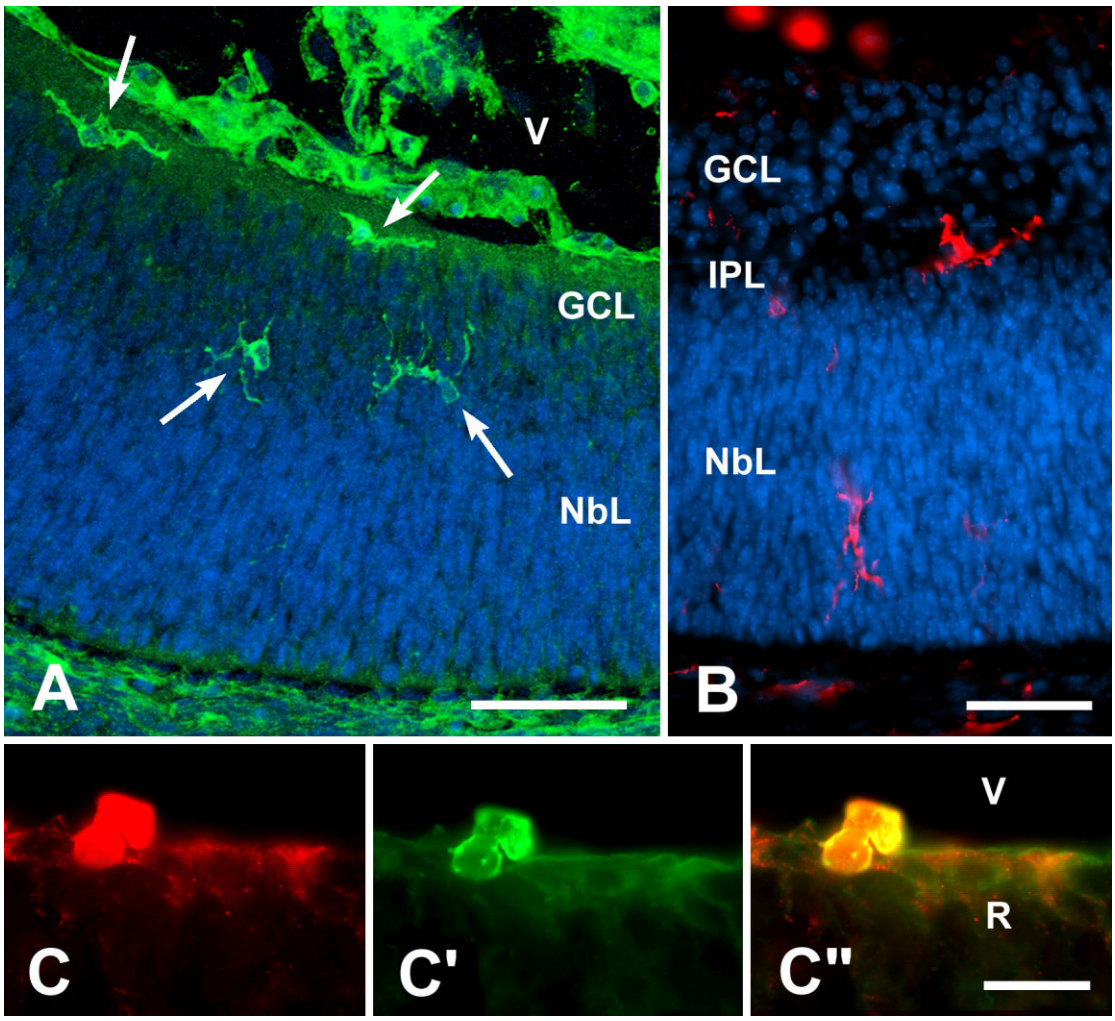

Fig. 3. Macrophage/microglial cells in mouse retinas at late embryonic development. **A:** Tomato lectin histochemical staining (green) of an E15.5 retina showing labeled microglial cells (arrows). Cell nuclei (blue) are stained with Hoechst. Hyaloid blood vessels within the vitreous (V) are also labeled. **B:** Iba1-immunopositive cells (red) in an E17.5 retina. Cell nuclei (blue) are stained with Hoechst. **C–C″:** A double-labeled cell with iba1 antibody (C, red) and tomato lectin (C′, green) (C″: merged, yellow-orange indicates double-stained structures) apparently traversing the border between retina (R) and vitreous (V) of an E18.5 eye. NbL, neuroblastic layer; IPL, inner plexiform layer; GCL, ganglion cell layer. Scale bars = 50 μm in A,B; 20 μm in C–C″.

than at P0 or P3, and virtually no microglial cells were seen across the vitreal border of the retina after P7. Microglial cell ramification progressively increased during the first postnatal week (Fig. 7A–C).

At the beginning of the second postnatal week the OPL could be distinguished in almost the entire retina. Microglial cells continued to be seen in the NFL, GCL, IPL, and INL. In general, microglial cells were frequently ramified in plexiform layers, whereas they were more compact in the INL and GCL. Thus, many microglial cells in the INL were radially oriented compact cells with processes reaching the IPL, where they ramified.

At the end of the second postnatal week all retinal layers were clearly demarcated throughout the retina and their general organization was similar to that seen in adult retinas. After the emergence of all retinal layers, microglial cells continued to be excluded from the ONL. In contrast, microglial cells were frequent in the contiguous OPL (Fig. 7D), where they had a ramified morphology, with most of their thin processes contained within the narrow limits of this layer. Microglial cells continued to be observed in the NFL, GCL, IPL, and INL, as described.

No modifications of the distribution pattern described at the end of the second postnatal week were observed during the following 2 weeks (P21 and P28 retinas). Usually, microglial cells in the plexiform layers of these retinas had an elaborated ramification pattern (Fig. 7E), with thin processes that sometimes entered the INL (Fig. 7F).

Microglial cells had a similar distribution in the adult retina to that described in retinas from P14 on. Thus, Iba1-positive microglial cells were located in the NFL, GCL, IPL, INL, and OPL (Fig. 8A). Most microglial cells showed an extensive ramification (Fig. 8B). As reported during postnatal development, no microglial cell bodies were observed within the ONL.

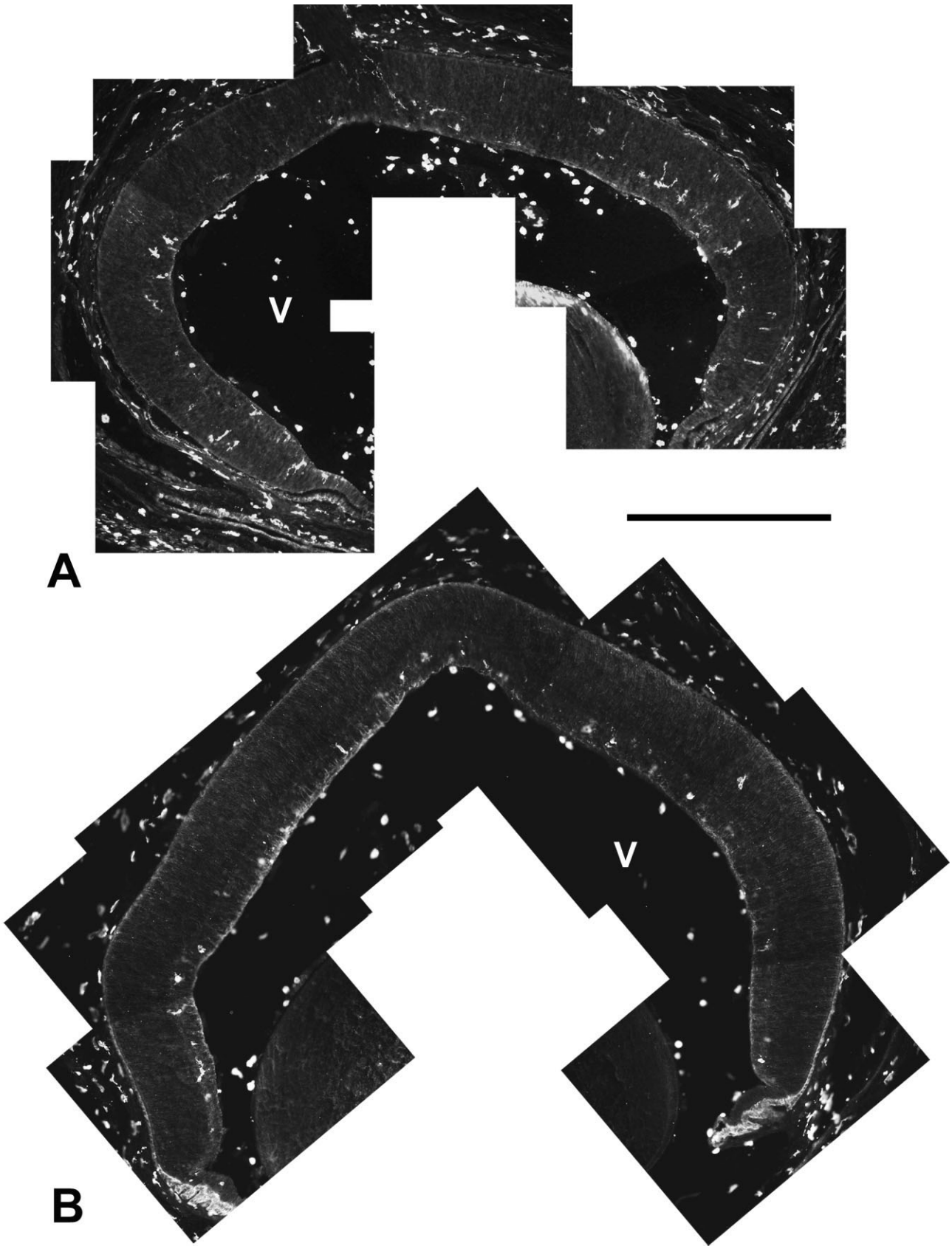

Fig. 4. Iba1-immunostained transverse sections of E17.5 (**A**) and P0 (**B**) mouse retinas showing the distribution of Iba1-positive macrophage/microglial cells in late embryonic and newborn retinas. Both sections were made with a temporal-to-nasal orientation at approximately the same level of the retina. Numerous labeled cells are seen in the E17.5 retina (A), whereas only a few are present at P0 (B). V, vitreous. Scale bar = 200 μm.

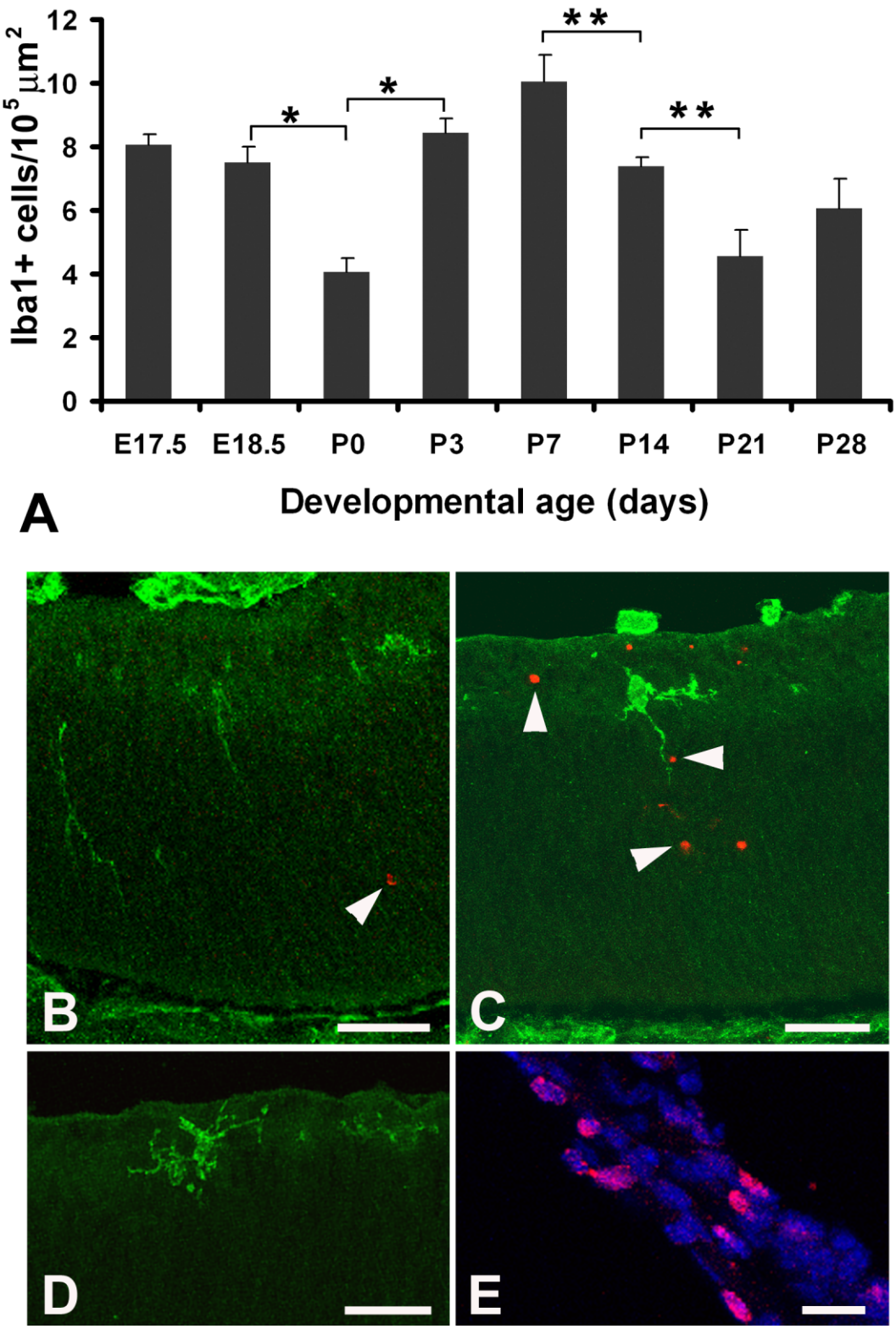

Fig. 5. Changes in microglial cell density during retinal development. **A:** Densities of Iba1-positive cells in the retina of mice at different embryonic and postnatal ages. Data are presented as means ± SEM of values obtained in at least four retinas at each age. Asterisks depict statistically significant differences between data from different stages (Student's *t*-test, $*P < 0.01$; $**P < 0.05$). **B,C:** TL (green) and TUNEL (red) double-labeled sections from E18.5 (B) and P0 (C) retinas. TL-labeled microglial cells do not show TUNEL-positive nucleus; arrowheads point out some TUNEL-positive bodies. **D,E:** Ki67 (red) labeled sections from P3 retina (D) and sclera (E). TL-positive microglial cells (green) do not show Ki67 staining in the retina (D), whereas some nuclei are Ki67-positive in the sclera, used as positive control. Cell nuclei are stained in E with Hoechst 33342. Scale bars = 30 μm.

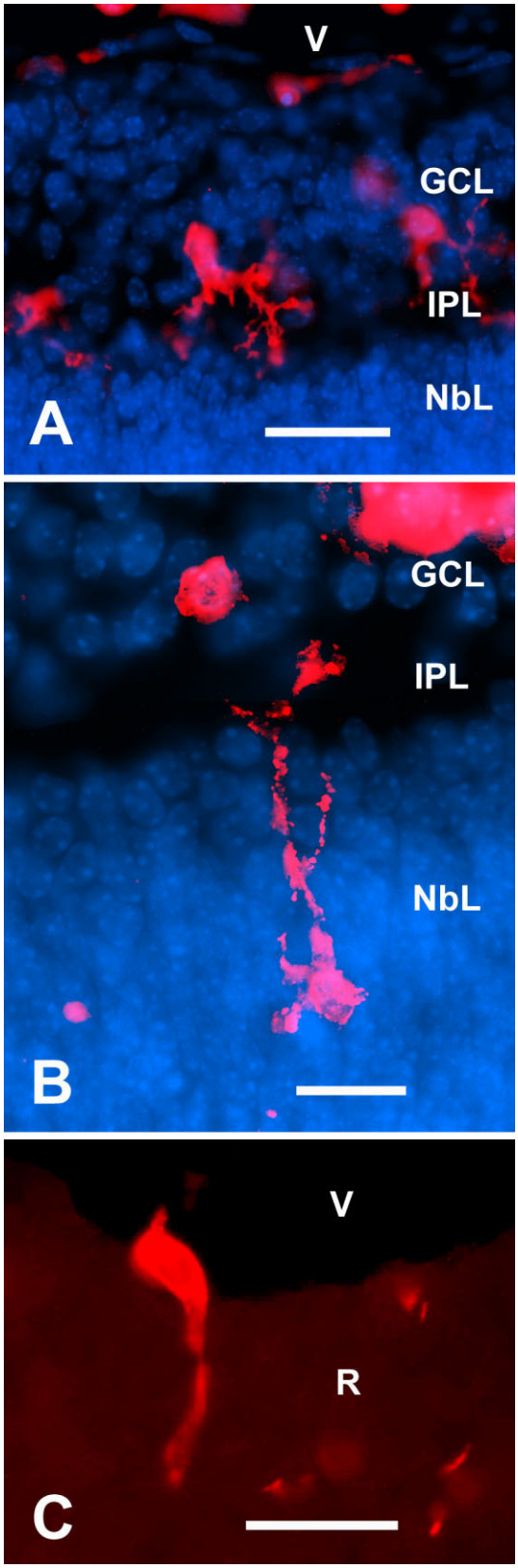

In summary, the mature pattern of microglial cell distribution in the mouse retina (as seen at adulthood) appeared to be attained during development at the same time as the mature layer organization of the retina, i.e., immediately after the emergence of the OPL during the second postnatal week. However, microglial cell density peaked at P7 and was significantly lower at P14 and P21 (Fig. 5). This may be explained by an increasing "dilution" of microglial cells within the retina due to progressive retinal growth combined with a stabilization of their number after entry of microglial precursors at the vitreal border ceased. The distribution of microglial cell bodies in the retina during postnatal development and adulthood is summarized in Figure 9. It can be seen that microglial cells appear only in the NFL/GCL region of the retina at P0, whereas they are present in the IPL and NbL at P3 and in the INL at P7. This distribution pattern suggests a radial migration from vitreal to deeper layers of the retina. It is noteworthy that some microglial cell bodies are present in the INL not only during developmental stages but also in the adult retina.

Differences in microglial distribution in the retina of pigmented and albino mouse retinas

The embryonic and postnatal development of retinal microglia described above was studied in pigmented mice. However, no evident differences could be observed between the distribution of microglia in the retina of pigmented (C57BL/6) and albino (BALB/c) mice, either during development or at adulthood (Fig. 10). Therefore, the changes in microglial distribution pattern during retina development reported above apply to both strains of mice.

DISCUSSION

The use of different microglial markers allows us to claim that most or even all retinal microglial cells were considered in our study, offering a complete view of the distribution of these cells in the developing and adult mouse retina.

Entry of macrophage/microglial cells into the retina

Macrophage/microglial cells are already present within the mouse retina at E11.5, the earliest stage studied here. Their morphological features and distribution are similar to those previously described during early embryonic development of rat (Ashwell et al., 1989) and avian (Cuadros et al., 1991) retinas. These cells seem to proceed from the vitreous and enter the neuroepithelium by traversing the vitreal surface of the retina, since numerous labeled cells are seen within the vitreous near the retinal region, which contains macrophage/microglial cells.

Fig. 6. Iba1-positive cells (red) in P0 mouse retinas. Retinal layers are distinguished in A and B by staining of cell nuclei with Hoechst (blue). **A:** Labeled cells within the developing ganglion cell layer (GCL) with processes reaching the immature inner plexiform layer (IPL). **B:** Immunolabeled cell with its soma located in the neuroblastic layer (NbL), from which a process emerges and reaches the IPL. **C:** Iba1-positive cell apparently traversing the border between the retina (R) and vitreous (V). Scale bars = 30 μm.

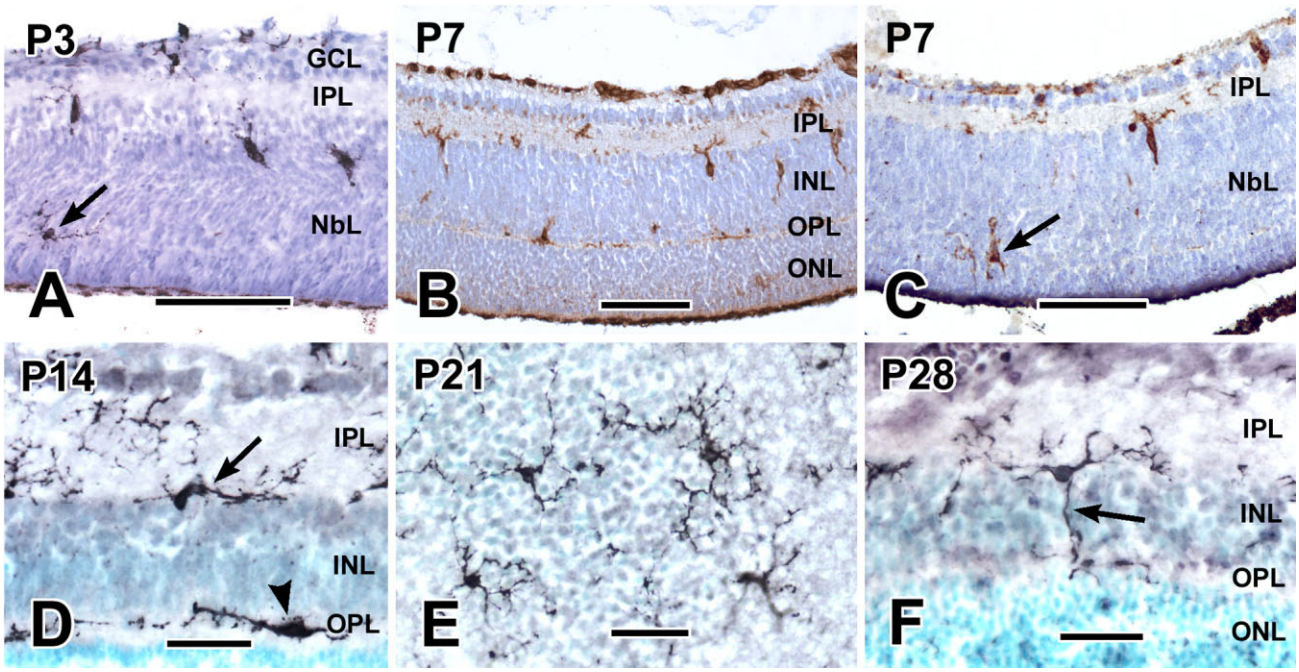

Fig. 7. Distribution of microglial cells in mouse retinas of different postnatal ages labeled with Iba1 immunostaining (A,D–F) or tomato lectin histochemistry (B,C). The label is visualized with peroxidase. **A:** Central part of a P3 retina showing Iba1-positive cells in neuroblastic layer (NbL) and ganglion cell layer (GCL). A labeled cell (arrow) is located in the region to be occupied by the future outer plexiform layer (OPL). IPL, inner plexiform layer. **B:** Central part of a P7 retina. A thin OPL containing microglial cells is discernible between the inner nuclear layer (INL) and outer nuclear layer (ONL). Abundant labeled cells are present in the INL, whereas no microglial cells are observed in the ONL, although labeling of some extracellular material can be seen in this layer. **C:** Peripheral region of the same P7 retina shown in B. The neuroblastic layer (NbL) contains labeled microglial cells, one of which (arrow) is seen in the region to be occupied by the still-undefined ONL. **D:** P14 retina. Iba1-labeled microglial cells show a well-ramified shape with most of their processes oriented horizontally. A microglial cell (arrow) is located in the border between the IPL and INL, whereas another (arrowhead) is contained in the OPL. **E:** P21 retina. Iba-1 labeled ramified microglial cells in a horizontal section at the level of the border between the IPL and INL. **F:** P28 retina. Iba1-immunolabeled microglial cell showing its soma and two of its processes in the border between the IPL and INL, whereas another process (arrow) traverses the inner nuclear layer and reaches the OPL, where it ramifies. Scale bars = 100 μm in A; 50 μm in B,C; 30 μm in D–F.

The amount of microglial cells within the retina increases from E12.5 until the end of embryonic development. During this period, labeled cells are observed close to the vitreal surface, apparently entering the retina. Microglial cells can also be seen in peripheral areas of mouse retina near the ciliary margin from E12.5 on. These observations suggest that microglial cells enter the embryonic retina via two routes: by crossing the vitreal surface of the retina and by migration from nonneural ciliary regions after crossing the peripheral margin of the retina. Entry of microglial cells across the ciliary margin has also been described in human and quail retinas (Diaz-Araya et al., 1995a; Provis et al., 1996; Marín-Teva et al., 1999b). Microglial cell entry by either route would contribute to increasing the number of microglial cells observed during embryonic development.

The density of microglial cells decreases at birth, raising questions about the fate of some of the microglial cells observed at the end of embryonic development. It can be suggested that the decrease in density may be a consequence of the increase in size of the early postnatal retina. Nevertheless, there are evident differences in the distribution of labeled cells between embryonic and postnatal retinas (see Fig. 4). Thus, far fewer microglial cells are present in the NbL of the newborn mouse retina than before birth. Therefore, microglial density appears to decrease not only because of the growth of retinal tissue but also as a consequence of the disappearance of some labeled cells. A similar decrease in microglial density at perinatal ages has also been described in rats (Ashwell et al., 1989) and rabbits (Ashwell, 1989). One plausible explanation for this disappearance could be the death of microglial cells, but TUNEL results ruled out this possibility. In this context, one study reported the presence of rare degenerating microglial cells in some regions of the developing rat brain and the apparent absence of any dying microglia in others (Dalmau et al., 2003), supporting the low frequency of cell death in the developing CNS of rodents. Egress of microglial cells from the retina may be involved in the decrease of microglial cell density at P0.

An important finding of our study was the increase in density of microglial cells in mouse retina during the first postnatal week, peaking at the end of this week and decreasing thereafter. Similar results were described in rat retina (Ashwell et al., 1989). Since no extensive proliferation of microglial cells was observed during the first postnatal week, the increase in microglial cell density between P0 and P7 would be related to the entry of new microglial cells into the retina. An indication of the migration of abundant microglial cells into the retina is the observation

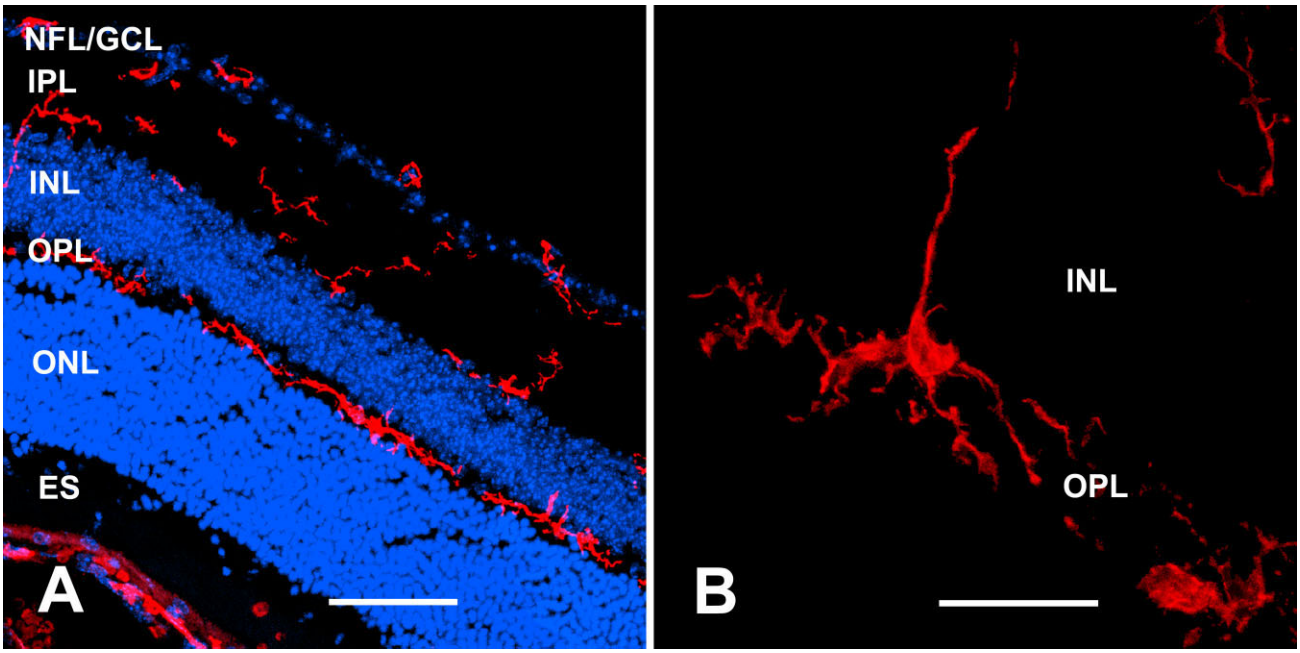

Fig. 8. Distribution of Iba1-immunolabeled microglia in adult (P60) retinas. **A:** Microglial cells are present in the nerve fiber layer/ganglion cell layer (NFL/GCL), inner plexiform layer (IPL), and outer plexiform layer (OPL) but not in the inner nuclear layer (INL) or outer nuclear layer (ONL). Hoechst staining of all nuclei reveals the retinal layers. ES, external segments of photoreceptor cells. **B:** Ramified microglial cell with its soma and horizontal processes in the OPL. A vertical process is seen in the INL. Scale bars = 50 μm in A; 20 μm in B.

at P0–7 of numerous labeled cells apparently crossing the vitreal border. By contrast, only a few labeled cells are seen entering the retina from the vitreous at stages older than P7, and the entry of a small number of microglial cells would not compensate for the marked growth of retinal tissue at these stages, explaining the decrease in microglial density.

It was previously proposed that microglial cells enter the retina from blood vessels before formation of the blood–retinal barrier (Thanos et al., 1996) and are related to cell death (Hume et al., 1983). However, no correlation was found between microglial entry and vascularization of the developing mouse retina in the present investigation. In fact, microglial cells were observed within the retina before its invasion by blood vessels (see Dorrell and Friedlander, 2006, for a review on mouse retina vascularization), ruling out direct entry of these cells via the blood. In support of the present findings, a previous study of the avascular retina of quail showed that microglial precursors colonized the retinal parenchyma despite the absence of blood vessels (Navascués et al., 1995). Our observations suggest that many microglial precursors in the mouse retina enter from the vitreous, which might be colonized by these precursors from the numerous blood vessels of the transient hyaloid vasculature that regresses at around the end of the second postnatal week (Ito and Yoshioka, 1999).

With respect to the possible relationship of cell death with microglial entry into the retina, dying cells are not frequent in mouse retinas between E15 and P1 (Pequignot et al., 2003), ages at which new microglial cells were observed within the retina. The entry of microglial cells in absence of cell death suggests that the two processes are independent. At perinatal stages, when numerous cells die in the mouse retina (Young, 1984), some microglial cells close to the vitreal border were in topographical relationship with dead cell fragments (not shown), but many others appeared to ignore dying cells in relatively close proximity.

Distribution pattern of retinal microglial cells during development and adulthood

Two different types of macrophage/microglial cells were found in the developing mouse retina. The first are macrophage-like cells present in the retina at E11.5 and E12.5, which appear to be related to cell death in the retinal region where optic axons exit to the optic nerve. The presence of cell death-related macrophage-like cells in the retina was previously described during the early development of mice (Rodríguez-Gallardo et al., 2005), other mammals (Knabe and Kuhn, 1999), and birds (Cuadros et al., 1991; Frade and Barde, 1998). From E12.5 on, other labeled cells that appear in the neural retina have a different morphology and no evident relationship with dead cell debris. It is therefore possible that two different waves of macrophage/microglial cells with distinct functional roles successively enter the retina during development, the first at E11.5–12.5 and the second from E12.5 on. This phenomenon is clearly seen in the quail retina, which contains macrophage-like cells between E3 and E5; these cells disappear at E6 before the retina is recolonized by cells that become microglia at E7 (Navascués et al., 1995). The distinction between two waves of invasion of the retina by macrophage-like cells and microglial precursors is more difficult to establish in mouse than in quail retina, since they appear to overlap in space and time, likely due to the smaller size of the mouse retina and its different development timetable. At any rate, the E13.5 retina con-

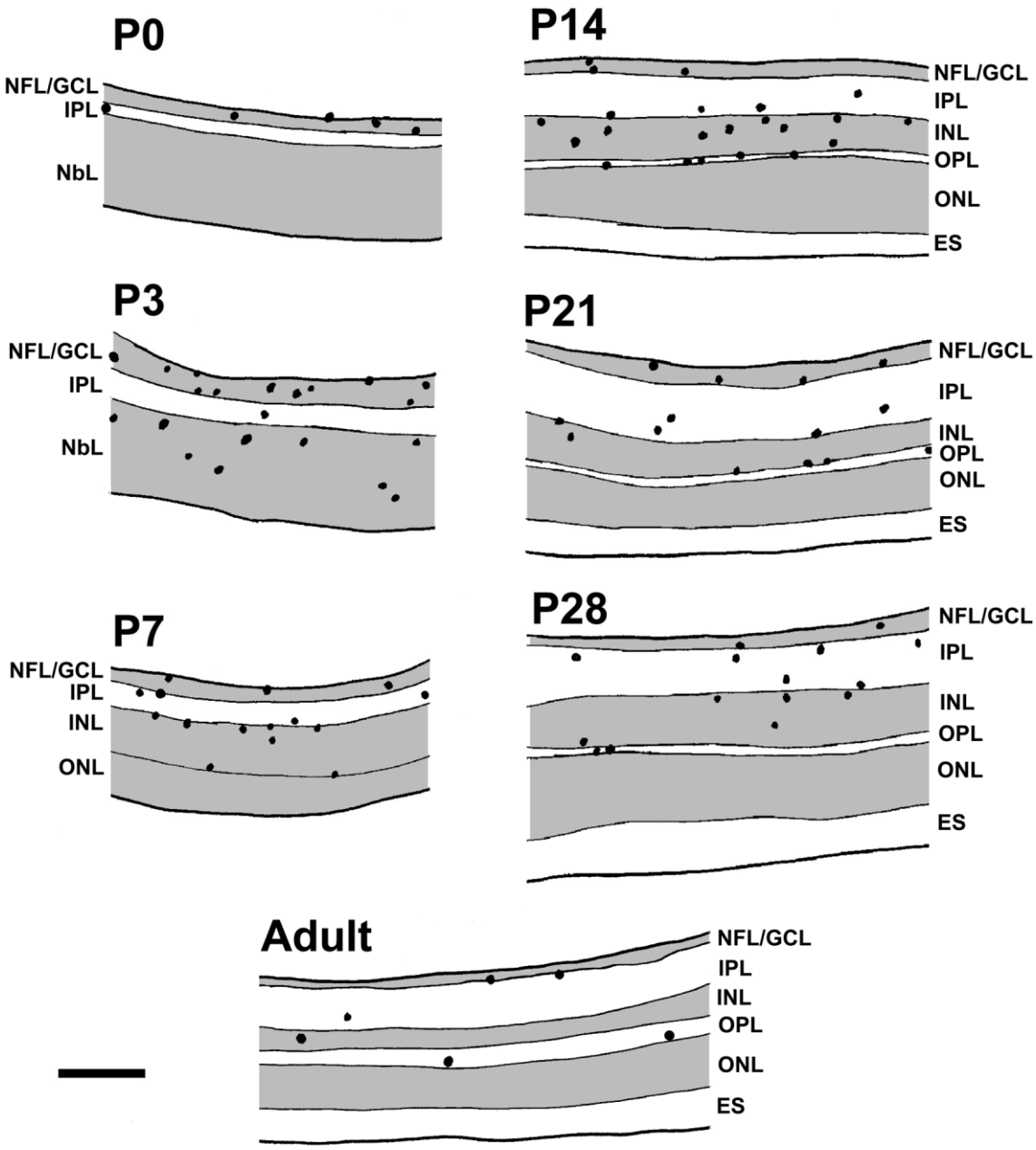

Fig. 9. Camera lucida drawings of Iba1-immunostained histological sections of mouse retinas at different ages from P0 to adulthood (indicated in each drawing) showing the location of microglial cell bodies (dots). Nuclear layers are shaded in gray. NFL/GCL, nerve fiber layer and ganglion cell layer; IPL, inner plexiform layer; INL, inner nuclear layer; OPL outer plexiform layer; ONL, outer nuclear layer; ES, external segments of photoreceptors; NbL, neuroblastic layer. Scale bar = 100 μm.

tains labeled cells that are probably microglial precursors, because their fate can be traced during development until the appearance of mature microglia.

Our results show that microglial cells are mainly restricted to vitreal layers immediately after birth but progressively appear at more scleral layers during the following days. Hence, it can be proposed that microglial cells move from vitreal toward scleral layers in a vitreal-to-scleral radial migration similar to that described in the developing quail retina (Navascués et al., 1995; Sánchez-López et al., 2004). In this migration microglial cells, first located at the NFL/GCL after their entry into the retina, successively colonize the IPL, INL, and OPL but do not enter the ONL. Microglial cells would progressively leave the NFL/GCL during their radial migration, explaining their lower numbers in these layers after P14, although some persist in the NFL/GCL until adulthood.

In adult mouse retina microglial cells are localized in the NFL, GCL, IPL, OPL, and occasionally in the INL, but

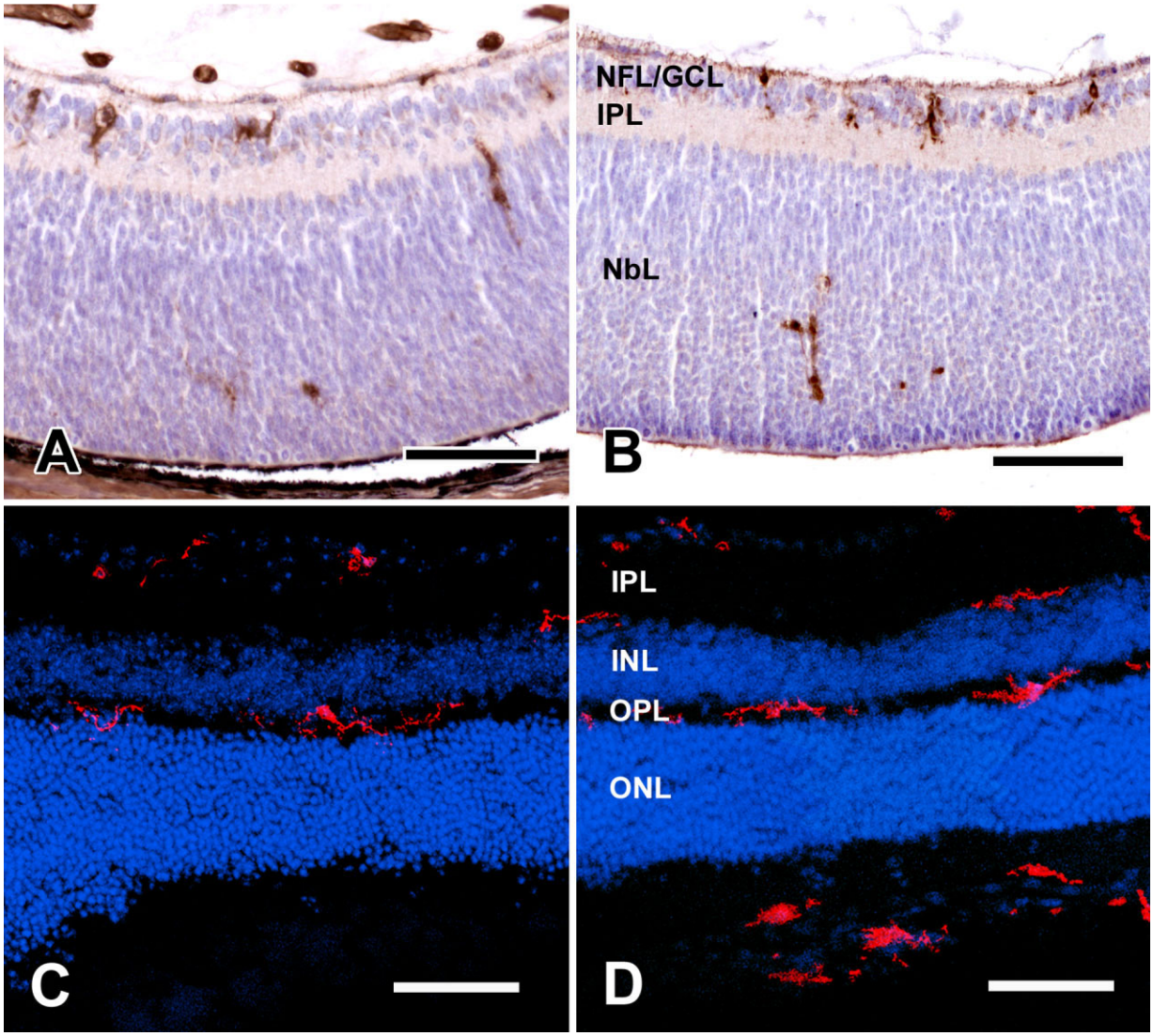

Fig. 10. Distribution of microglial cells in transverse sections of pigmented (C57BL/6 strain, A,C) and albino (BALB/c strain, B,D) retinas. **A,B:** Microglial cells stained with tomato lectin histochemistry revealed by immunoperoxidase in P3 retinas. **C,D:** Confocal images showing the distribution of microglial cells in adult (P60) retinas as revealed by Iba1 immunostaining (red); nuclear Hoechst stain (blue) reveals the localization of retinal layers. Microglial distribution is similar in both strains during development (A,B) and at adulthood (C,D). NFL/GCL, nerve fiber layer and ganglion cell layer; IPL, inner plexiform layer; INL, inner nuclear layer; OPL outer plexiform layer; ONL, outer nuclear layer; NbL, neuroblastic layer. Scale bars = 75 μm in A,B; 50 μm in C,D.

no microglial cells are seen in the ONL, although some microglial processes can occasionally be observed in this layer. This distribution pattern is similar to previous reports on various species (Schnitzer, 1989; Navascués et al., 1994; Harada et al., 2002; Hughes et al., 2003). Although the presence of microglial cells in the OPL of some species has been debated (see Schnitzer, 1989), our results clearly demonstrate their presence in the OPL of the mouse retina, as reported in birds (Navascués et al., 1994; Sánchez-López et al., 2004) and rabbits (Schnitzer, 1989). We highlight the presence of some microglial cell bodies in the INL of the adult mouse retina, contrasting with descriptions in quail retina, in which microglial cells are seen in the INL during development but not at adulthood (Navascués et al., 1994; Marín-Teva et al., 1999c).

Our results cannot confirm the existence of microglial cell tangential migration from the center toward the periphery in mouse retina beyond any reasonable doubt. The morphological features of microglial cells around the optic disc suggest that they move from the center to the periphery of the retina. Nevertheless, no microglial invasion front demarcating microglia-containing areas from microglia-free areas was seen at any stage of retinal development. Therefore, irrefutable evidence was not obtained of central-to-peripheral tangential migration of microglial cells, which has been demonstrated in birds

(Navascués et al., 1995; Marín-Teva et al., 1999c). Differences in microglial migration pattern between mammalian and avian retinas would not be surprising, given the marked differences in the vascularization pattern of the retina and vitreous between the two animal groups. Thus, in the avian eye, blood vessels are not present in the retina and the vitreous but are collected in a vascular organ, the pecten, which appears early in development and projects into the vitreous in the central region of the eye; microglial precursors migrate tangentially from this central region. By contrast, during development of the mouse eye hyaloid vessels are present in the vitreous close to the surface of the entire retina. The present study revealed that many macrophage-lineage cells localized among hyaloid vessels in the vitreous cross the vitreal border during the first postnatal week to become microglia in the retina. This entry of microglial precursors from the vitreous appears to take place at any point on the retinal surface; therefore, no migration from a specific region would be necessary for microglial precursors to colonize the entire retina.

Our study reveals no differences in the distribution pattern of microglial cells between pigmented (C57Bl/6) and albino (Balb/c) mouse retinas either during development or adulthood. Other authors reported that the number of macrophage/microglial cells appearing in the subretinal space differed between pigmented and nonpigmented strains of mice during the first postnatal week (Ng and Streilein, 2001). We cannot rule out that careful quantitative studies might reveal some differences in the number of microglial cells in the retina between albino and pigmented mice. Therefore, although the two strains of mouse can be indistinctly used for studies on the general distribution of microglial cells in the retina, further research is required to establish whether there are any differences in the number of microglial cells in the retinas of these strains.

The proposition that the topographical distribution of cell death contributes to shaping the distribution of microglia (Hume al., 1983; Wong and Hughes, 1987) is not corroborated by the present observations, since no relationship could be established between the distribution of cell death (Pequignot et al., 2003) and that of microglial cells in mouse retina. Thus, these cells appear within the INL before extensive cell death occurs in this layer. Likewise, other authors reported that microglial cells migrated toward regions showing cell degeneration in pathological retinas (Thanos, 1992; Thanos et al., 1996; Gupta et al., 2003). Again, no relationship was found between the distribution of microglia and the development of blood vessels within the retina. Moreover, microglial cells are present in the avascular retina of birds (Navascués et al., 1995) and in regions of the rabbit retina that lack blood vessels (Schnitzer, 1989). In developing human retinas, establishment of microglial topography has been described as occurring in two phases, one that is independent from vascularization and a second associated with the development of retinal vessels (Diaz-Araya et al., 1995a). An alternative view has been suggested by a recent report that development of the retinal vasculature is dependent on the presence of microglial cells, since normal retinal vessels do not develop when the microglial cell population is depleted (Checchin et al., 2006).

The migration and distribution of microglial cells in the retina may be influenced by other factors. Thus, microglial cells in the developing quail retina migrate by adhering to Müller cell processes (Marín-Teva et al., 1998; Sánchez-López et al., 2004), and the extracellular molecule tenascin appears to regulate microglial cell ramification (Sánchez-López et al., 2004). However, similar mechanisms have yet to be elucidated in the mouse retina.

ACKNOWLEDGMENTS

We thank Richard Davies for improving the English style of the article.

LITERATURE CITED

Acarin L, Vela JM, González B, Castellano B. 1994. Demonstration of poly-N acetyl lactosamine residues in ameboid and ramified microglial cells in rat brain by tomato lectin binding. J Histochem Cytochem 42:1033–1041.

Aloisi F. 2001. Immune function of microglia. Glia 36:165–179.

Ashwell K. 1989. Development of microglia in the albino rabbit retina. J Comp Neurol 287:286–301.

Ashwell KW, Hollander H, Streit W, Stone J. 1989. The appearance and distribution of microglia in the developing retina of the rat. Vis Neurosci 2:437–448.

Boycott BB, Hopkins JM. 1981. Microglia in the retina of monkey and other mammals: its distinction from other types of glia and horizontal cells. Neuroscience 6:679–688.

Checchin D, Sennlaub F, Levavasseur E, Leduc M, Chemtob S. 2006. Potential role of microglia in retinal blood vessel formation. Invest Ophthalmol Vis Sci 47:3595–3602.

Chen L, Yang P, Kijlstra A. 2002. Distribution, markers, and functions of retinal microglia. Ocul Immunol Inflamm 10:27–39.

Cuadros MA, García-Martín M, Martin C, Ríos A. 1991. Hemopoietic phagocytes in the early differentiating avian retina. J Anat 177:145–158.

Cuadros MA, Navascués J. 1998. The origin and differentiation of microglial cells during development. Prog Neurobiol 56:173–189.

Cuadros MA, Martin C, Coltey P, Almendros A, Navascues J. 1993. First appearance, distribution, and origin of macrophages in the early development of the avian central nervous system. J Comp Neurol 330: 113–129.

Cuadros MA, Santos AM, Martín-Oliva D, Calvente R, Tassi M, Marín-Teva JL, Navascués J. 2006. Specific immunolabeling of brain macrophages and microglial cells in developing and mature chick central nervous system. J Histochem Cytochem 54:727–738.

Da Silva RP, Gordon S. 1999. Phagocytosis stimulates alternative glycosylation of macrosialin (mouse CD68), a macrophage-specific endosomal protein. Biochem J 338:687–694.

Dalmau I, Vela JM, González B, Finsen B, Castellano B. 2003. Dynamics of microglia in the developing rat brain. J Comp Neurol 458:144–157.

Diaz-Araya CM, Provis JM, Penfold PL, Billson FA. 1995a. Development of microglial topography in human retina. J Comp Neurol 363:53–68.

Diaz-Araya CM, Provis JM, Penfold PL. 1995b. Ontogeny and cellular expression of MHC and leukocyte antigens in human retina. Glia 15:458–470.

Dorrell MI, Friedlander M. 2006. Mechanisms of endothelial cell guidance and vascular patterning in the developing mouse retina. Prog Ret Eye Res 25:277–295.

Dowding AJ, Maggs A, Scholes J. 1991. Diversity amongst the microglia in growing and regenerating fish CNS: immunohistochemical characterization using FL.1, an anti-macrophage monoclonal antibody. Glia 4:345–364.

Frade JM, Barde YA. 1998. Microglial-derived nerve growth factor causes cell death in the developing retina. Neuron 20:35–41.

Garcia-Valenzuela E, Sharma SC, Pina AL. 2005. Multilayered retinal microglial response to optic nerve transection in rats. Mol Vis 11:225–231.

Goodbrand IA, Gaze RM. 1991. Microglia in tadpoles of Xenopus-laevis — normal distribution and the response to optic nerve injury. Anat Embryol 184:71–82.

Gupta N, Brown KE, Milam AH. 2003. Activated microglia in human retinitis pigmentosa, late-onset retinal degeneration, and age-related macular degeneration. Exp Eye Res 76:463–471.

Harada T, Harada C, Kohsaka S, Wada E, Yoshida K, Ohno S, Mamada H, Tanaka K, Parada LF, Wada K. 2002. Microglia-Muller glia cell inter-

actions control neurotrophic factor production during light-induced retinal degeneration. J Neurosci 22:9228–9236.

Herbomel P, Thisse B, Thisse C. 2001. Zebrafish early macrophages colonize cephalic mesenchyme and developing brain, retina, and epidermis through a M-CSF receptor-dependent invasive process. Dev Biol 238: 274–288.

Hughes EH, Schlichtenbrede FC, Murphy CC, Sarra GM, Luthert PJ, Ali RR, Dick AD. 2003. Generation of activated sialoadhesin-positive microglia during retinal degeneration. Invest Ophthalmol Vis Sci 44: 2229–2234.

Hume DA, Gordon S. 1983. Mononuclear phagocyte system of the mouse defined by immunohistochemical localization of antigen F4/80. Identification of resident macrophages in renal medullary and cortical interstitium and the juxtaglomerular complex. J Exp Med 157:1704–1709.

Hume DA, Perry VH, Gordon S. 1983. Immunochemical localization of a macrophage-specific antigen in developing mouse retina: phagocytosis of dying neurons and differentiation of microglial cells to form a regular array in the plexiform layers. J Cell Biol 97:253–257.

Humphrey MF, Moore SR. 1996. Microglial responses to focal lesions of the rabbit retina: correlation with neural and macroglial reactions. Glia 16:325–341.

Ito M, Yoshioka M. 1999. Regression of the hyaloid vessels and pupillary membrane of the mouse. Anat Embryol 200:403–411.

Ito D, Imai Y, Ohsawa K, Nakajima K, Fukuuchi Y, Kohsaka S. 1998. Microglia specific localisation of a novel calcium binding protein, Iba1. Mol Brain Res 57:1–9

Knabe W, Khun HJ. 1999. The earliest invasion of macrophages into the developing brain and eye of the tree shrew *Tupaia belangeri*. Anat Embryol 200:393–402.

Kreutzberg GW. 1996. Microglia: a sensor for pathological events in the CNS. Trends Neurosci 19:312–318.

Lawson LJ, Perry VH, Dri P, Gordon, S. 1990. Heterogeneity in the distribution and morphology of microglia in the normal adult mouse brain. Neuroscience 39:151–170.

Mallat M, Marín-Teva JL, Cheret C. 2005. Phagocytosis in the developing CNS: more than clearing the corpses. Curr Opin Neurobiol 15:101–107.

Marín-Teva JL, Almendros A, Calvente R, Cuadros MA, Navascués J. 1998. Tangential migration of ameboid microglia in the developing quail retina: mechanism of migration and migratory behavior. Glia 22:31–52.

Marín-Teva JL, Almendros A, Calvente R, Cuadros MA, Navascués J. 1999a. Proliferation of actively migrating ameboid microglia in the developing quail retina. Anat Embryol 200:289–300.

Marín-Teva JL, Calvente R, Cuadros MA, Almendros A, Navascués J. 1999b. Circumferential migration of ameboid microglia in the margin of the developing quail retina. Glia 27:226–238.

Marín-Teva JL, Cuadros MA, Calvente R, Almendros A, Navascués J. 1999c. Naturally occurring cell death and migration of microglial precursors in the quail retina during normal development. J Comp Neurol 412:255–75.

Mittelbronn M, Dietz K, Schluesener HJ, Meyermann R. 2001. Local distribution of microglia in the normal adult human central nervous system differs by up to one order of magnitude. Acta Neuropathol 101:249–255

Navascués J, Moujahid A, Quesada A, Cuadros MA. 1994. Microglia in the avian retina: immunocytochemical demonstration in the adult quail. J Comp Neurol 350:171–186.

Navascués J, Moujahid A, Almendros A, Marín-Teva JL, Cuadros MA. 1995. Origin of microglia in the quail retina: central-to-peripheral and vitreal-to-scleral migration of microglial precursors during development. J Comp Neurol 354:209–228.

Ng TF, Streilein JW. 2001. Light-induced migration of retinal microglia into the subretinal space. Invest Ophthalmol Vis Sci 42:3301–3310.

Nimmerjahn A, Kirchhoff F, Helmchen F. 2005. Resting microglial cells are highly dynamic surveillants of brain parenchyma in vivo. Science 308: 1314–1318.

Penfold PL, Madigan MC, Provis JM. 1991. Antibodies to human leucocyte antigens indicate subpopulations of microglia in human retina. Vis Neurosci 7:383–388.

Penfold PL, Madigan MC, Gillies MC, Provis JM. 2001. Immunological and aetiological aspects of macular degeneration. Prog Ret Eye Res 20:385–414.

Penninger JM, Irie-Sasaki J, Sasaki T, Oliveira-dos Santos AJ. 2001. CD45: new jobs for an old acquaintance. Nat Immunol 2:389–396.

Pequignot MO, Provost AC, Salle S, Taupin P, Sainton KM, Marchant D, Martinou JC, Ameisen JC, Jais JP, Abitbol M. 2003. Major role of BAX in apoptosis during retinal development and in establishment of a functional postnatal retina. Dev Dyn 228:231–238.

Provis JM, Penfold PE, Edwards AJ, Van Driel D. 1995. Human retinal microglia: expression of immune markers and relationship to the *glia limitans*. Glia 14:243–256.

Provis JM, Diaz CM, Penfold PL. 1996. Microglia in human retina: a heterogeneous population with distinct ontogenies. Perspect Dev Neurobiol 3:213–222.

Rodríguez-Gallardo L, Lineros-Domínguez MC, Francisco-Morcillo J, Martín-Partido G. 2005. Macrophages during retina and optic nerve development in the mouse embryo: relationship to cell death and optic fibres. Anat Embryol 210:303–316.

Roque RR, Imperial CJ, Caldwell RB. 1996. Microglial cells invade the outer retina as photoreceptors degenerate in Royal College of Surgeons rats. Invest Ophthalmol Vis Sci 37:196–203.

Salvador-Silva M, Vidal-Sanz M, Villegas-Pérez MP. 2000. Microglial cells in the retina of Carassius auratus: effects of optic nerve crush. J Comp Neurol 417:431–447.

Sánchez-López A, Cuadros MA, Calvente R, Tassi M, Marín-Teva JL, Navascués J. 2004. Radial migration of developing microglial cells in quail retina: a confocal microscopy study. Glia 463:261–273.

Sánchez-López A, Cuadros MA, Calvente R, Tassi M, Marín-Teva JL, Navascués J. 2005. Activation of immature microglia in response to stab wound in embryonic quail retina. J Comp Neurol 492:20–33.

Schlüter C, Duchrow M, Wohlenberg C, Becker MHG, Key G, Flad HD, Gerdes J. 1993. The cell proliferation-associated antigen of antibody Ki-67: a very large, ubiquitous nuclear protein with numerous repeated elements, representing a new kind of cell cycle-maintaining proteins. J Cell Biol 123:513–522

Schnitzer J. 1989. Enzyme-histochemical demonstration of microglial cells in the adult and postnatal rabbit retina. J Comp Neurol 282:249–263.

Stoll G, Jander S. 1999. The role of microglia and macrophages in the pathophysiology of the CNS. Prog Neurobiol 58:233–247.

Streit WJ, Walter SA, Pennell NA. 1999. Reactive microgliosis. Prog Neurobiol 57:563–581.

Thanos S. 1992. Sick photoreceptors attract activated microglia from the ganglion cell layer: a model to study the inflammatory cascades in rats with inherited retinal dystrophy. Brain Res 588:21–28

Thanos S, Moore S, Hong YM. 1996. Retinal microglia. Prog Ret Eye Res 15:331–361.

Vrabec FR. 1970. Microglia in the monkey and rabbit retina. J Neuropathol Exp Neurol 29:217–224.

Won MH, Kang TC, Cho SS. 2000. Glial cells in the bird retina: immunochemical detection. Microsc Res Tech 50:151–160.

Wong RO, Hughes A. 1987. Role of cell death in the topogenesis of neuronal distributions in the developing cat retinal ganglion cell layer. J Comp Neurol 262:496–511.

Yamato S, Hirabayashi Y, Sugihara H. 1984. An improved procedure for the histochemical demonstration of cathepsin D by the mercury-labeled pepstatin method. Stain Tech 59:113–120.

Yang P, Das PK, Kijlstra A. 2000. Localization and characterization of immunocompetent cells in the human retina. Ocul Immunol Inflam 8:149–157.

Young RW. 1984. Cell death during differentiation of the retina in the mouse. J Comp Neurol 229:362–373

Zhang C, Lam TT, Tso MO. 2005a. Heterogeneous populations of microglia/macrophages in the retina and their activation after retinal ischemia and reperfusion injury. Exp Eye Res 81:700–709.

Zhang C, Shen JK, Lam TT, Zeng HY, Chiang SK, Yang F, Tso MO. 2005b. Activation of microglia and chemokines in light-induced retinal degeneration. Mol Vis 11:887–895.